

Plasmonic meta-screen for alleviating the trade-offs in the near-field optics

Yan Wang, Alex M. H. Wong, Loïc Markley, Amr S. Helmy
and George V. Eleftheriades*

*The Edward S. Rogers Sr. Department of Electrical and Computer Engineering
University of Toronto
40 St. George Street
Toronto, Ontario, Canada, M5S 2E4
gelefh@waves.utoronto.ca

Abstract: We propose a “meta-screen” design, consisting of a metallic sheet patterned with a dense array of nano-sized slot antennas, for inducing sub-wavelength optical spots in the near-field. Compared to other transmission screen topologies, our design overcomes the trade-off of low throughput versus resolution of a sub-wavelength aperture by inducing resonance in the slots. In addition, the antenna array serves to effectively narrow the spot size through the superposition of spatially shifted beams produced by each slot element. Such a design offers a practical approach for extending the near-field sensing/imaging distance at optical frequencies. The effectiveness of narrowing the spot size through the array topology is demonstrated by evaluating the full-width-half-maximum (FWHM) beamwidth at a distance of $0.1\lambda_0$ away from the screen. We show that an array with just three elements improves the beamwidth by more than 30% compared to a single resonant slot element. In this paper, important issues such as the operating principle and the design process of the meta-screen, the characteristics of plasmonic slot antenna, the impact of the number of array elements, and the effect of asymmetry due to the presence of a supporting substrate are discussed.

©2009 Optical Society of America

OCIS codes: (050.6624) Subwavelength structures; (310.6628) Subwavelength structures, nanostructures; (250.5403) Plasmonics; (050.1220) Apertures; (180.4243) Near-field microscopy.

References and links

1. E. G. Bortchagovsky, S. Klein, and U. C. Fischer, “Surface plasmon mediated tip enhanced Raman scattering,” *Appl. Phys. Lett.* **94**(6), 063118 (2009).
2. N. Fang, H. Lee, C. Sun, and X. Zhang, “Sub-diffraction-limited optical imaging with a silver superlens,” *Science* **308**(5721), 534–537 (2005).
3. E. Cubukcu, E. A. Kort, K. B. Crozier, and F. Capasso, “Plasmonic laser antenna,” *Appl. Phys. Lett.* **89**(9), 093120 (2006).
4. E. X. Jin, and X. Xu, “Plasmonic effects in near-field optical transmission enhancement through a single bowtie shaped aperture,” *Appl. Phys. B* **84**(1-2), 3–9 (2006).
5. T. H. Taminiau, R. J. Moerland, F. B. Segerink, L. Kuipers, and N. F. van Hulst, “ $\lambda/4$ resonance of an optical monopole antenna probed by single molecule fluorescence,” *Nano Lett.* **7**(1), 28 (2007).
6. H. J. Lezec, A. Degiron, E. Devaux, R. A. Linke, L. Martin-Moreno, F. J. Garcia-Vidal, and T. W. Ebbesen, “Beaming light from a subwavelength aperture,” *Science* **297**(5582), 820–822 (2002).
7. A. Grbic, L. Jiang, and R. Merlin, “Near-field plates: subdiffraction focusing with patterned surfaces,” *Science* **320**(5875), 511 (2008).
8. L. Markley, A. M. H. Wong, Y. Wang, and G. V. Eleftheriades, “A spatially shifted beam approach to subwavelength focusing,” *Phys. Rev. Lett.* **101**(11), 113901 (2008).
9. L. Novotny, “Effective wavelength scaling for optical antennas,” *Phys. Rev. Lett.* **98**(26), 266802 (2007).
10. A. Alú, and N. Engheta, “Tuning the scattering response of optical nanoantennas with nanocircuit loads,” *Nat. Photonics* **2**(5), 307–310 (2008).
11. G. V. Eleftheriades, and A. M. H. Wong, “Holography-inspired screens for sub-wavelength focusing in the near field,” *IEEE Microw. Wireless Compon. Lett.* **18**(4), 236 (2008) (Resonant version).

1. Introduction

Focusing optical waves with sub-wavelength resolution enables many disciplines such as near-field microscopy, spatially resolved spectroscopy and photolithography. Sub-wavelength focusing is commonly achieved by transmitting light through single sub-wavelength apertures, which are usually on the order of a few tens of nanometers in size in order to achieve the desired spot size. This sub-wavelength focusing scheme entails a trade-off between the resolution, which is represented by the spot size, and the attenuation imposed by the small aperture on the optical fields. Overcoming this trade-off can enhance numerous applications, and in particular those which rely on an intense field, such as the tip-enhanced Raman spectroscopy [1]. The emerging field of negative refraction metamaterials is one route which holds significant promise to alleviate this trade-off [2]. However, the successful demonstrations of negative refraction to date have been narrow band, and have involved lossy optical structures which would not improve the light throughput in comparison to conventional single sub-wavelength apertures.

Classical diffraction theory dictates that a single sub-wavelength aperture placed on an opaque screen transmits light inefficiently, and isotropically diffracts light in the space after the aperture. This dictates that for us to obtain sub-wavelength resolution, an operating distance of a small fraction of the operating wavelength is essential. This in turn leads to cumbersome setups, which are challenging to stabilize and use widely. Increasing the operating distance of this scheme would greatly enhance its use and extends the applications which it enables.

The low transmission efficiency in near-field optics can be improved through modifying characteristics of the apertures, such as altering their shapes to induce resonances. Under resonance conditions, a given aperture's transmission and directivity can be significantly enhanced. For example, when an aperture is operated at half-wavelength resonance, it forms a classical half wavelength slot antenna with radiated field amplitude larger than that of the excitation and an enhanced directivity. At optical frequencies, strong resonances can be induced by utilizing surface plasmon modes at metal-dielectric interfaces. Such plasmon modes exist due to the degradation in the metals' opacity with increasing frequencies. Antennas based on plasmonic resonances have recently shown remarkable performance for transmission enhancement in the near-field [3–5]. These techniques are all inspired by the concepts of antenna designs at microwave frequencies, and exploit the resonance effect in a single aperture only. Another technique proposed for enhancing the resonance condition and controlling the directivity of transmission utilizes concentric gratings to surround the sub-wavelength aperture [6]. This technique is only suited for far-field applications since the large grating period destroys the near-field profile. In order to improve upon the current aperture antenna techniques available for near-field optical applications, the need still exists for structures that can improve performances over single aperture antennas. The solution also needs to be simpler to realize and design in comparison to those offered via negative refraction metamaterials. In this paper, we propose and analyze a design, which achieves these goals in comparison to existing research [4,5].

We propose a planar structure that overcomes the trade-offs associated with sub-wavelength aperture designs by relying on resonances in the apertures, as well as the array concepts inspired by microwave antenna arrays. The design uses a metallic "meta-screen" that consists of a dense array of slot antennas. Resonances are induced and tuned through the slots' location and size. More specifically, the tuning produces opposite phase in successive apertures that sharpens the transmitted beam through interference. As a result, the slot array serves to narrow the spot size in the near-field beyond the sub-diffraction ability of a single aperture, while the resonance condition enables extraordinary transmission. This design scales a sub-wavelength focusing technique originally proposed for the microwave regime to the optical domain, thereby offering unprecedented opportunities for adapting other radio-

frequency (RF) antennas and antenna-array concepts for nano-optics applications. This technique, which is based on near-field interference is especially valuable for the nano-optics community since many focusing designs in the microwave regime cannot be scaled easily to the optical regime due to their complicated structures (for example [7]).

Some preliminary results of translating the meta-screen design from the microwave to the optical domain are briefly presented in the supplementary material of [8] without outlining any design details. In this paper, we give a thorough analysis on the behavior of plasmonic antennas and the meta-screen at optical frequencies, and highlight how such a design can alleviate the trade-offs associated with the near-field optics.

2. Antenna design implementation in the optical regime

Despite the lack of well developed methodologies for designing optical antennas and arrays compared to their microwave counterparts, recent studies such as [3–5] have revealed the feasibility of implementing such structures. Furthermore, it is shown that the effective wavelength can be estimated more systematically using a linear scaling law in the optical frequency range [9]. More recently, nano-circuit elements have also been proposed for loading and tuning the frequency responses of antennas [10].

Antennas such as a half-wavelength dipole and a slot at microwave frequencies have a physical length close to the half wavelength of the excitation. However, their optical counterparts exhibit a shorter physical length due to the smaller effective wavelength of the surface plasmon modes along the antenna arms [9]. In addition, the thickness of the metallic screen is negligible at microwave frequencies, but become significant in the optical range given that the metal becomes more translucent. This will have implications on the transmitted fields as will be discussed below. As such, the task of adapting a meta-screen at microwave frequencies to the optical domain translates to designing a plasmonic antenna array with equivalent weights for their elements. Such a weighted array profile is also referred to as the transmission pattern.

To demonstrate the benefits of operating at resonance, a plasmonic slot antenna of 40nm wide on a silver screen of 40nm thick is analyzed at 830nm operating wavelength. The effective wavelength of the slot antenna is investigated by numerically determining its physical length using the commercial software Comsol Multiphysics. As shown in Fig. 1, the observed maximum transmission occurs at 200nm for the given operating wavelength. This slot length corresponds to the effective half-wavelength of this structure. This result matches with the observation in [9], where the effective wavelength of its complimentary structure (i.e. a silver dipole antenna of 20nm radius) is found to be approximately 400nm.

As mentioned before, besides the physical length, another important difference between the microwave and plasmonic slot antennas is that a thin plasmonic screen permits evanescent tunneling of the incident plane wave due to the translucency of metals at optical frequencies. This has implications on the transmitted fields as depicted in Fig. 2, where the comparison between the field transmission of an ideal perfect-electric-conductor (PEC) and a plasmonic slot antenna with corresponding effective half-wavelength is conducted. The figure shows that the transmitted fields for the plasmonic slot antenna is a superposition of the plane-wave tunneled through the thin plasmonic screen and the slot radiation, which produces a standing wave interference pattern. The interference decreases as the thickness of the screen increases. In the case presented here, the 40 nm silver screen thickness renders the background “leakage” small compared to the radiation due to slot resonance. However the significance of the metal film thickness is evident.

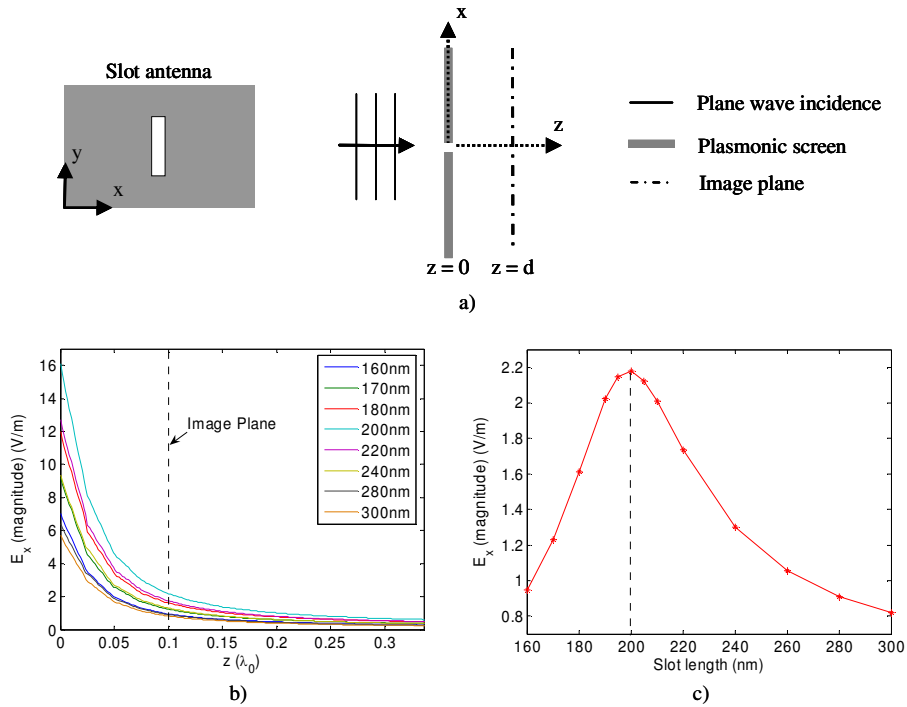


Fig. 1. Field transmission for a plasmonic slot antenna when subjected to a plane wave incidence with magnitude of 1V/m and $\lambda_0 = 830\text{nm}$. Light passes through the slot and a diffracted beam is formed on the other side. The width of the beam changes depending on the location of the image plane. The slot width and the metal screen thickness are both 40nm in our analysis. (a) The operation of a plasmonic slot antenna. (b) The transmitted field through the slot antennas of various lengths. (c) The magnitude of E_x vs. the slot length at the image plane located at $0.1\lambda_0$ away from the transmission screen.

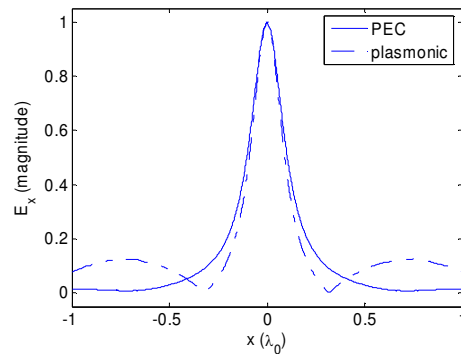


Fig. 2. Comparison of the normalized diffraction patterns at the image plane ($0.1\lambda_0$ away from the plasmonic screen) due to a single slot antenna on a perfect-electric-conductor (PEC) and a plasmonic screen. The slot has a width of 40nm. The PEC screen is infinitesimally thin and the plasmonic screen has a thickness of 40nm. The standing wave pattern observed for the plasmonic slot antenna is due to the interference of the plane-wave leakage and the slot radiation.

Finally, the practical realization of these structures dictates that the silver film is deposited on a thick dielectric substrate instead of being suspended in air. This results in asymmetric media on each side of the meta-screen. Therefore, the design has to be modified to account for

the asymmetry. In our simulation, the substrate is placed at the incident half-plane. The substrate material in our structure is silica glass with an electric permittivity of 2.09. The effect of asymmetry, as illustrated in Fig. 3, leads to a further reduction of the antenna resonance length. This is due to a shorter effective wavelength of the surface mode supported at the silica glass and silver interface. Figure 3(b) also shows that this reduced effective wavelength is in between the ones for symmetric media of the air (the blue curve) and the silica glass (the red curve), because the maximum transmission occurs when optimal coupling is achieved between the two asymmetric surface modes.

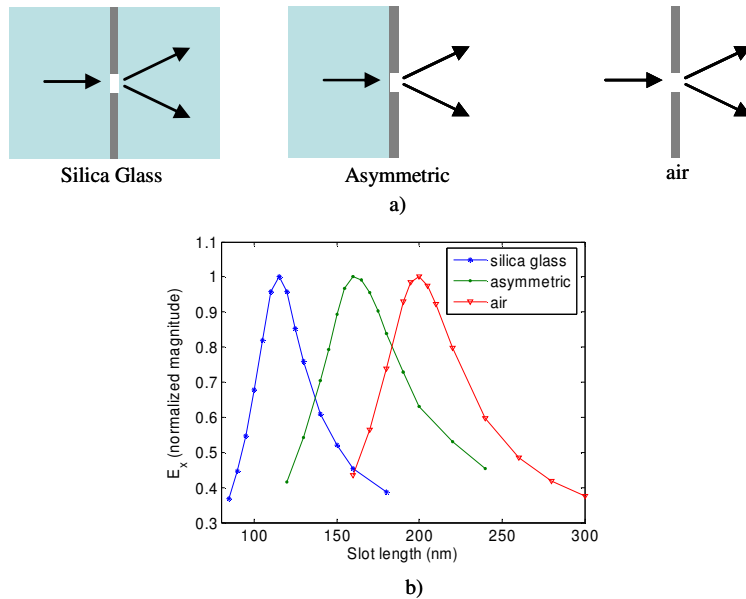


Fig. 3. The effect of varying the incidence and the transmission media on the resonance wavelength of the slot antenna. (a) Operation of a slot antenna in various incidence and transmission media. (b) The effective resonance wavelengths (i.e. double of the slot lengths) for the three scenarios above are 230nm, 320nm and 400nm respectively.

3. Background theory of metal slot arrays

The structure of “meta-screen” is illustrated in Fig. 4, where the incident light is transmitted and diffracted through an array of symmetrically distributed slot antennas on a metallic screen. Through an example that compares the diffraction patterns of the light transmitted through one slot and three slots in Fig. 5, the reduction in the width of the light beam due to the array interference is clearly evident. This near-field beamwidth reduction topology has been analyzed at microwave frequencies from two perspectives. The first uses near-field holography analysis, where the *backward propagation method* is applied to the spectrum of a desired beamwidth at the image plane in order to derive the corresponding field pattern at the transmission screen [11,12]. The various radiating elements of a slot antenna array are then designed according to such a transmission pattern. The second approach investigates the near-field interference of an array of radiating elements, where the phase retardation of the far-field is replaced by a spatial offset (spatially shifted beams [8]). The weights of the radiating elements are derived through the *method of moments* for the best-fit of the desired beam shape. Both methods aim to find the weights (both the magnitude and the phase) of each radiating element.

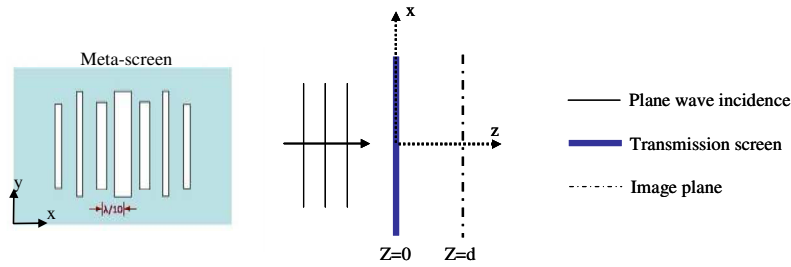


Fig. 4. The operation of the meta-screen. The meta-screen is a thin metallic screen with a series of slots of varying geometries. The separation distance between the slots is subwavelength, and in this case, it is fixed at $0.1\lambda_0$. A plane wave is incident from one side of the meta-screen and a diffracted beam is formed on the other side. The slot patterns are designed to produce a desired (sub-wavelength) beam pattern on the image plane located in the near-field.

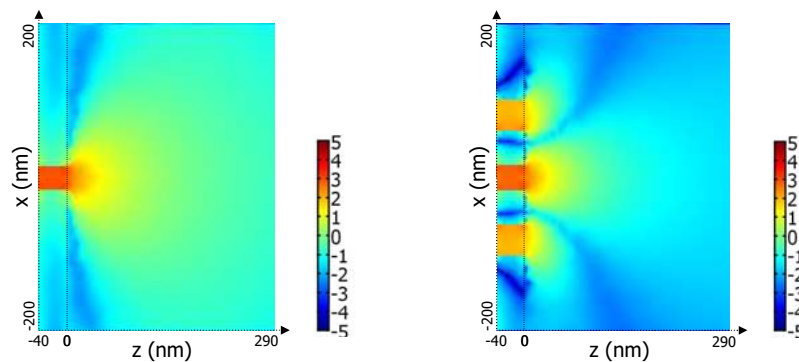


Fig. 5. Comparison of the field transmission for a meta-screen with single and triple-slot antennas. This is the top-view of the field strength (in logarithmic scale) in the transmission half-plane, where the weighted 3-slot array provides more confinement of the light beam. In these simulations, the plasmonic screen is 40nm thick and the antennas are all 40nm wide. The length of the single resonant antenna in (a) and the central slot antenna in (b) is 200nm. The satellite antennas in (b) have a length of 130nm. The wavelength of excitation is 830nm and the separation distance between the slots is 83nm.

The chief distinctions between the “meta-screen” approach discussed in this work for enhancing the directivity and those which use conventional antenna-array concepts in the far-field are a) the operation in the near field; b) the use of unequal (non periodic) slot elements; c) the special choice of the amplitudes and phases that the slots excite; and d) the sub-wavelength spacing between slots. More specifically, the near-field operation leads to a spatial shift (instead of a phase retardation in the far-field) for a source when it changes location [8]. The amplitude and the phase of the slot array are weighted through altering the geometry of its individual elements rather than creating a feed network. In fact, the phase between adjacent slots is effectively reversed due to the unequal length of the slots. This results in destructive interference that leads to a sharper beamwidth [8]. The sub-wavelength separation distance between successive slots gives rise to the name “meta-screen”. It is worth noting that the sub-wavelength slot separation also results in strong mutual coupling among the antenna elements. This mutual coupling presents a design challenge because the collective behavior of the antenna array is very different from the superposition of its individual elements. Therefore, the dimensions of the slots that produce desired weights do not lead to the expected beamwidth at the image plane. As a result, the slot dimensions have to be fine tuned extensively in order to satisfy the beamwidth requirement. Finally, since the spacing between adjacent slots determines the largest transverse wavenumber of the higher order

evanescent wave excited by the meta-screen, this sub-wavelength separation ultimately determines the resolution according to the Nyquist theorem.

This near-field approach leads to some remarkable and attractive features. Ideally, an infinite number of slots are needed to produce the desired beamwidth at any near-field locations. However, depending on the near-field distance and the spot size of interest, a few slots can provide a remarkably close approximation. One example is the one dimensional field profile of Fig. 5 at $z = 0.1\lambda_0$, which is shown in Fig. 6(a). As can be clearly seen in the figure, we are able to produce a Gaussian beam with a FWHM of $0.12\lambda_0$ using as few as three elements when the image plane is $0.1\lambda_0$ away from the transmission screen. However, if we would like to produce the same beamwidth at $0.25\lambda_0$, the 3-slot array is insufficient because it only achieves a FWHM of $0.22\lambda_0$ as illustrated in Fig. 6(b). One way to overcome this limitation is to add more slots on the transmission screen. As can also be seen in Fig. 6(b), a 9-slot array can achieve a FWHM of $0.14\lambda_0$ [8].

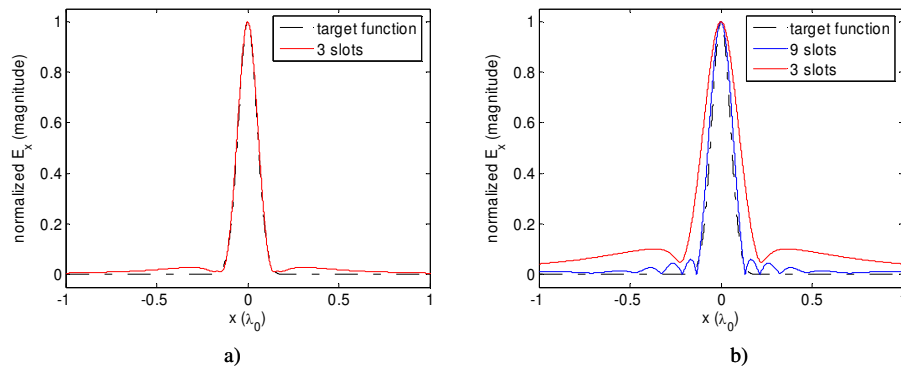


Fig. 6. The effect of the number of slots on the approximation of a desired beamwidth. (a) The FWHM is $0.12\lambda_0$ for the 3-slot array when the image plane is at $z = 0.1\lambda_0$. (b) The FWHM is $0.14\lambda_0$ for the 9-slot array, and $0.22\lambda_0$ for the 3-slot array when the image plane is at $z = 0.25\lambda_0$.

The option of maintaining the sub-wavelength spot size at increasing distances from the metal screen by using more array elements provides a powerful design tool for near-field optics. This feature in combination with extraordinary transmission is very useful for sensing, lithography and other near-field applications because we cannot achieve the same performance by using just a single sub-wavelength aperture. The multiple slot design is easy to implement in the optical regime, where advanced nano-fabrication techniques can be used to realize the slot features.

4. Translating the meta-screen from the microwave to the optical domain

In this section, we use a three-slot meta-screen as an example to illustrate that this topology is feasible at optical frequencies, and that the concept of using an antenna-array can produce a much more superior result than just a single resonant slot. In this example, the image plane is $0.1\lambda_0$ away from the transmission screen and the desired image beam pattern is illustrated in Fig. 7(a). Note that despite having the same FWHM beamwidth, the target beam in Fig. 6(a) is a normalized Gaussian function, whereas the one in Fig. 7(a) is a truncated point source whose evanescent spectrum contains up to $5k_0$. As shown in [11], this corresponds to the spacing between the slots. The choice of the target function is arbitrary, we only need to choose one with ample evanescent components so that the beamwidth is smaller than the one of a single slot. In this case, we use the image in Fig. 7(a) because we can make a direct comparison with the microwave frequency results presented in [11].

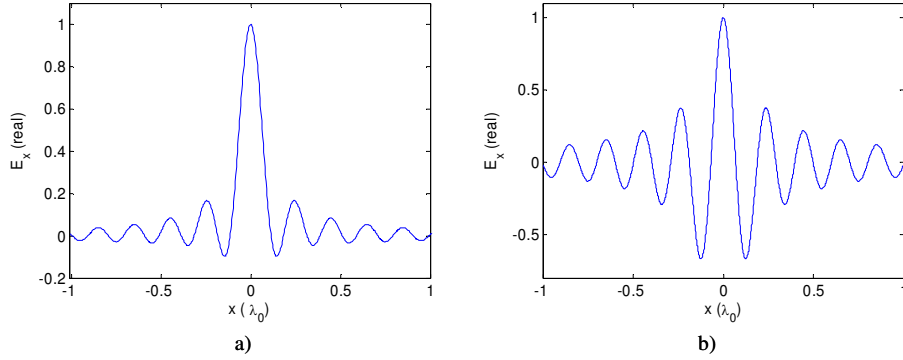


Fig. 7. An example of a given target beam at the image plane and the derived corresponding transmission field pattern. (a) Target field. (b) Transmission field. The target field is a point source with a truncated spectrum that contains up to $5k_0$, and a FWHM of $0.12\lambda_0$. The image plane is $0.1\lambda_0$ away from the transmission screen.

By applying the backward propagation analysis to the spectrum of Fig. 7(a), the corresponding transmission pattern is derived and illustrated in Fig. 7(b). Then by sampling the transmission pattern with intervals of $0.1\lambda_0$ (the separation distance of the slots), the approximated weights of the slot fields are $E_x = 1, -1/2, 1/5, -1/10, \dots$ symmetrically distributed with respect to $x = 0$. The number of slots can be chosen for desired accuracy. Here, we choose three slots to show that just a few elements can give a good approximation to the desired beamwidth. Finally, the weights of the slots are achieved by altering the slot geometries according to Fig. 1. The central slot is chosen to have a half wavelength resonance of 200nm in order to maximize the transmission, and two satellite slots with length of 130nm are placed on each side of the central slot to create desired near-field interference.

The effect of enhanced confinement due to such an antenna array compared to a single slot resonance is demonstrated in Fig. 8(b). The FWHM at the near-field distance of $0.1\lambda_0$ away from the screen is $0.115\lambda_0$ for the triple-slot transmission pattern, which is a 37% improvement compared to $0.182\lambda_0$ for a single-slot in *Comsol* fullwave simulations. We can see that the 3-slot array approximates the desired beamwidth in Fig. 8(a) very well, similar to what was observed at microwave frequencies. In order to highlight the importance of the phase reversal in adjacent slots, simulations were carried out for an array, where all three slots are in phase. As can be seen in Fig. 8(b), the scattered beam from each slot adds up and produces an even wider beam than just a single resonant antenna. Finally, small discrepancies between the diffraction patterns in Fig. 8(a) and 8(b) exist because the analysis is carried out based on the assumption of a perfect-electric-conductor transmission screen of an infinitesimal thickness (Fig. 8(a)), which is clearly not the case for our plasmonic screen (Fig. 8(b)). Nonetheless, our results confirm that the meta-screen topology provides the desired beam-sharpening effect at optical frequencies. More importantly, we can visualize the enhanced confinement at other near-field distances from Fig. 9(a). This further attests to the capability of these structures to effectively extend the near-field operating distance of a single resonant aperture.

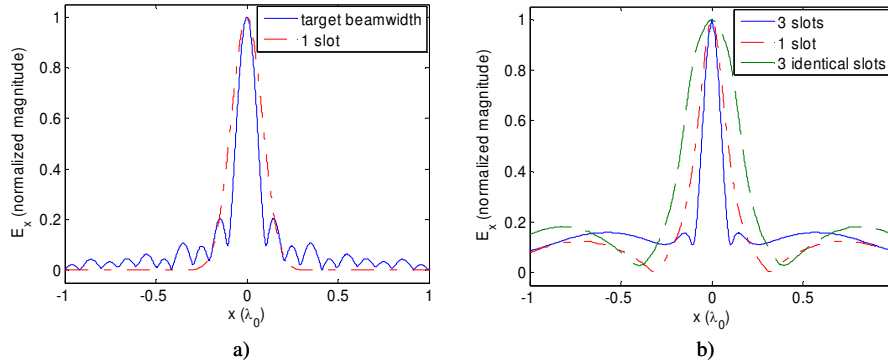


Fig. 8. Beamwidth reduction utilizing a meta-screen. (a) Theoretical beamwidth reduction at $0.1\lambda_0$ away for a PEC transmission screen. The FWHM of the target beamwidth and the diffraction of a single slot antenna are $0.12\lambda_0$ and $0.2\lambda_0$ respectively. We expect a 40% improvement for this best case scenario, which can be achieved with an infinite number of slots. (b) Simulated beamwidth reduction at $0.1\lambda_0$ away for a plasmonic transmission screen. The corresponding beamwidths due to a weighted 3-slot array of unequal lengths, a single plasmonic antenna, and an unweighted 3-slot array of equal lengths, are $0.115\lambda_0$, $0.182\lambda_0$, and $0.33\lambda_0$ respectively. The beamwidth reduction is due to the destructive interference from the satellite slots. Therefore, the weighted 3-slot array that produced opposite phase in successive array elements shows 37% improvement from a single slot. On the other hand, the array with three elements of equal length (200nm) produces fields that are in phase in all slots, which in turn widens the beamwidth even further.

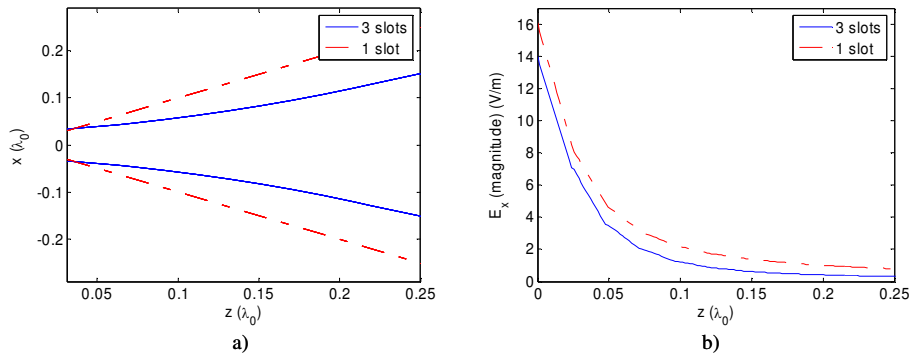


Fig. 9. Comparison of a triple-slot plasmonic meta-screen and a single resonant slot antenna. (a) Diffracted beamwidths away from the transmission screen at various image plane locations. (b) Comparison of the field transmission for a single resonant slot antenna and a triple-slot antenna array ($x, y = 0$).

5. Discussion

The advantages of the meta-screen technique in near-field optics can be better appreciated when directly compared to single sub-wavelength circular apertures. It is instructive to note that improving the resolution via the monotonic reduction of the single aperture size is only possible if the operating distance is not a concern. For example, if we want to achieve our target beamwidth ($0.12\lambda_0$) at a sensing distance of $0.1\lambda_0$ from the screen, it is not possible when only using a subwavelength hole. This is because the high-spatial components generated by the small circular aperture decay more rapidly, so it is not possible to enable this resolution at such a distance. As illustrated in Fig. 10(a), when we shrink the aperture diameter from 160nm down to 20nm, the beamwidth at our image plane does not improve much beyond a certain size (40nm diameter in our case), whereas the 3-slot meta-screen can produce a much sharper beam. It is also worth mentioning that we assume perfect electric conductor for

simulations involving small holes because the tunneling of the incident plane wave through the thin plasmonic screen overpowers the weak scattered field from the small hole. This finding further proves the limitations associated with single apertures. Therefore, achieving a given spot size using a meta-screen not only provides the enhanced transmission associated with the resonant central aperture as illustrated in Fig. 10(b), but also extends the operating distance via the use of satellite slots to reduce the beam size.

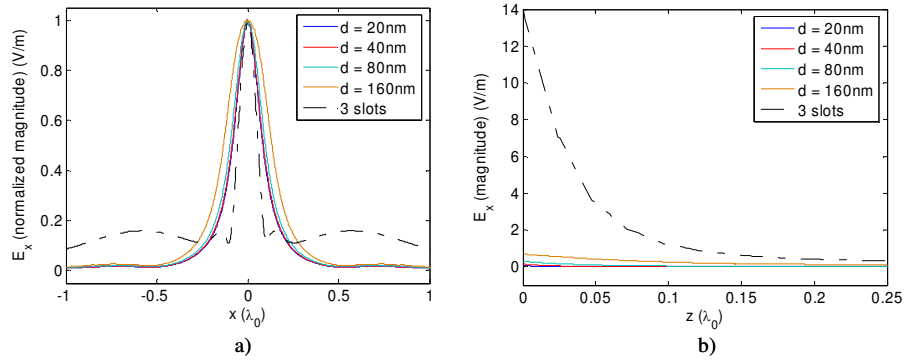


Fig. 10. Comparison of a triple-slot meta-screen and a single sub-wavelength circular aperture of various diameters. (a) Comparison of the beamwidth for a sub-wavelength circular aperture and a triple-slot array. (b) Comparison of the transmitted field strength for a sub-wavelength circular aperture and a triple-slot array.

We mentioned previously that adding a substrate in the incident domain decreases the effective resonant wavelength of plasmonic antennas. It in turn affects the geometry of our slot antenna array as well as their mutual couplings. Therefore, we have to redesign our antenna array to account for such changes. The new design consists of a central slot and two satellite slots with a length of 160nm and 110nm respectively while maintaining the same thickness and width as before. The length of the central slot is the resonant half-wavelength for the asymmetric incidence/transmission media described in Fig. 3. The satellite slot length is once again found by fine-tuning the slot geometry, so that the desired beamwidth is achieved at the image plane. The result in Fig. 11 shows a 33% improvement compared to a single resonant antenna in the same asymmetric setting.

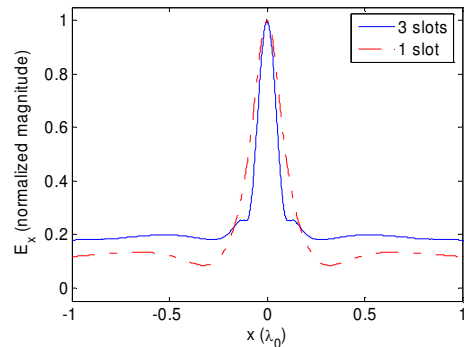


Fig. 11. Simulated beamwidth at $0.1\lambda_0$ away from the transmission screen for the silver meta-screen deposited on silica glass substrate. The FWHMs are $0.123\lambda_0$ and $0.183\lambda_0$ respectively.

6. Conclusion

In conclusion, we demonstrate that the “meta-screen” structure consisting of an array of plasmonic slot antennas can be used to achieve highly confined sub-diffraction focusing in the near-field. The implementation of the meta-screen at optical frequencies shows the advantage

of its structural simplicity compared to other super-focusing techniques. The benefit of the multiple radiating elements over a single resonant aperture plasmonic antenna is illustrated by comparing their near-field diffraction beamwidth. More specifically, the FWHM beamwidth due a three-slot array shows more than 30% reduction compared to a single resonating slot antenna at an image plane $0.1\lambda_0$ away from the transmission screen. The reduction is more significant with increasing operating distance in the near-field. Since the separation distance between each element is sub-wavelength, these multi-slot designs do not occupy large areas for patterning. In our case, the total area that the 3-slot array occupies is only 260×200 nm, and the slot dimensions are amenable to be realized using current nanofabrication technologies. Finally, this design can be modified to operate at other near-field distances by altering the number of slots and their geometries, as well as the separation distance to achieve desired beamwidths.